ELSEVIER

Chemical Geology 184 (2002) 123–138

CHEMICAL GEOLOGY
INCLUDING
ISOTOPE GEOSCIENCE

www.elsevier.com/locate/chemgeo

Zircon trace element geochemistry: partitioning with garnet and the link between U–Pb ages and metamorphism

Daniela Rubatto *

Research School of Earth Sciences, The Australian National University, Mills Road, Canberra ACT, 0200 Australia

Received 12 January 2001; accepted 23 July 2001

Abstract

With the aim to link zircon composition with paragenesis and thus metamorphic conditions, zircons from eclogite- and granulite-facies rocks were analysed for trace elements using LA-ICP-MS and SHRIMP ion microprobe. Metamorphic zircons from these different settings display a large variation in trace element composition. In the granulites, zircon overgrowths formed in equilibrium with partial melt and are similar to magmatic zircon in terms of high Y, Hf and P content, steep heavy-enriched REE pattern, positive Ce anomaly and negative Eu anomaly. They are distinguishable from magmatic zircon because of their low Th/U ratio. Independently of whole rock composition, metamorphic zircon domains in eclogite-facies rocks have low Th/U ratio and reduced HREE enrichment and Eu anomaly. In a low grade metamorphic vein, zircon has low Th/U ratio but is extremely enriched in Y, Nb and HREE.

Petrological and geochronological data demonstrate that metamorphic zircon overgrowths crystallised at granulite-facies conditions in equilibrium with unzoned garnet. It is thus possible for the first time to calculate trace element distribution coefficients between zircon and garnet. Hf is the elements that most strongly partition into zircon. Y, Nb and REE have distribution coefficients between 90 and 0.9 with minimum values for the MREE.

In eclogite-facies rocks, the HREE depletion in metamorphic zircon domains is attributed to concurrent formation of garnet under sub-solidus conditions. In one sample, the zircon/garnet trace elements partitioning indicates that metamorphic zircon formed in equilibrium with the garnet rim, i.e. at the eclogitic peak. The reduced Eu anomaly in the metamorphic zircon is interpreted as indicating absence of feldspars and thus supports zircon formation in eclogite facies.

In a metamorphic vein within the eclogite-facies rocks, zircons have larger Eu anomaly with respect to high-pressure zircon. Together with geochronological evidence, the Eu anomaly suggests that these zircons formed during prograde metamorphism, before the break down of feldspars at high pressure.

The REE composition of zircon can therefore relate zircon formation to specific metamorphic stages such as eclogite, granulite or greenschist facies. This allows linking zircon U–Pb ages with pressure–temperature conditions, a fundamental step in constraining rates of metamorphic processes.

Keywords: Zircon; Trace elements; Distribution coefficients; Metamorphism; Eclogite; Granulite

1. Introduction

Radioisotope geochronology is the principal technique by which the absolute ages of geological

* Fax: +61-2-6125-0738.
E-mail address: daniela.rubatto@anu.edu.au (D. Rubatto).

0009-2541/02/$ - see front matter
PII: S0009-2541(01)00355-2

processes can be determined. A common approach to the geochronological investigation of rocks that have had a complex thermal evolution is dating via isotopic systems that have a high closure temperature, such as U–Pb in zircon (Lee et al., 1997; Cherniak and Watson, 2001). The development of high mass resolution ion microprobes (e.g., SHRIMP) allows in-situ measurements of U–Pb ages of growth zones within single crystals, which may record different stages of the rock history. One of the main limitations of U–Pb geochronology has now become the lack of knowledge regarding the geological significance of the various mineral growth zones that can be dated. Unlike other minerals used for geochronology, such as garnet, micas or titanite, very little is known about the response of zircon to metamorphism. Recent studies have established that zircon can (re)crystallise over a wide range of pressure and temperature conditions, during prograde (Fraser et al., 1997; Liati and Gebauer, 1999), retrograde (Roberts and Finger, 1997; Rubatto et al., 2001) or peak metamorphism (Rubatto et al., 1998, 1999; Liati and Gebauer, 1999; Hoskin and Black, 2001). As metamorphism can last over millions to tens of millions of years, it is a fundamental requirement to relate zircon growth with specific pressure and temperature conditions in order to interpret U–Pb ages accurately and obtain rates of metamorphic processes.

Mineral inclusions in zircon provide a direct link between zircon formation and metamorphism (e.g., Gebauer et al., 1997; Hermann et al., 2001), but they are rare. The few previous attempts to relate zircon growth to metamorphic reactions (Roberts and Finger, 1997; Scoates and Chamberlain, 1997) have been limited by zircon-forming reactions being dependent upon the whole rock composition and hence any conclusion is restricted to a limited number of rock types. Moreover, this approach is not feasible in the case of recrystallisation of pre-existing crystals. A third, and more direct approach, is to obtain information on metamorphic conditions directly from the composition of zircon itself.

Zircon trace element geochemistry has been used previously to investigate the composition of parental melts (Hinton and Upton, 1999; Barbey et al., 1995) or the provenance of zircon crystals (Heaman et al., 1990; Maas et al., 1992; Paterson et al., 1992; Hoskin and Ireland, 2000). The application of zircon trace element geochemistry to metamorphic environments, however, is limited to a few studies dealing with high-temperature (HT) metamorphic rocks (Peucat et al., 1995; Schaltegger et al., 1999; Hoskin and Black, 2000). It has been suggested that the REE composition of zircon reflects, at least in some cases, the concurrent growth of minerals such as garnet (depletion in HREE; Schaltegger et al., 1999), monazite (depletion in LREE; Peucat et al., 1995) or feldspars (negative Eu anomaly; Murali et al., 1983; Peucat et al., 1995). It appears therefore possible that the trace element composition and the REE patterns of zircon can monitor the coexisting paragenesis.

The present paper considers the possible direct links between zircon composition and metamorphic conditions, knowledge of which would greatly improve the way we can date metamorphism by U–Pb. To investigate this possibility, zircon has been studied from granulitic migmatites and eclogite-facies rocks in which metamorphic zircon formation is well documented. In both cases, the presence or absence of minerals such as garnet, monazite and feldspars plays an important role: granulitic migmatites always contain feldspar as a melt phase, contain monazite, and garnet is often present in the paragenesis; eclogite-facies rocks never contain feldspars, monazite is generally absent, and garnet is always present. Further, the composition of zircon from the two environments is different, a pre-requisite in order to successfully investigate variation in zircon geochemistry with paragenesis. The granulite-facies case represents an ideal setting in which to study zircon geochemistry in an ‘open’ system with an infinite reservoir of trace elements—the melt—and to measure zircon/garnet partitioning. Metamorphic zircon in the eclogite-facies rocks is believed to have formed under sub-solidus conditions, in the absence of melt. We present contrasting cases of fluid fluxed crystallisation and ‘closed’ system recrystallisation of pre-existing crystals with a limited reservoir of trace elements, i.e. the reacting whole rock.

2. Methods

Zircon trace element analyses were performed on the SHRIMP II ion microprobe at the Research School of Earth Sciences (RSES), Canberra and on the LA-

ICP-MS at both the RSES and the ETH in Zürich. For SHRIMP, energy filtering was applied to reduce molecular interferences. Whenever possible, two isotopes for each REE were measured so that the isotopic ratios could be used to check for isobaric interferences. Detection limits for a pit 40 μm across and a few micrometers deep were in the order of 0.01 ppm. Details of the operating conditions and data reduction have been described by Hoskin (1998).

LA-ICP-MS analyses at the RSES (Eggins et al., 1998) used a pulsed 193-nm ArF Excimer laser with 100 mJ energy at a repetition rate of 5 Hz. A mixed He–Ar stream transported the aerosol into the ICP-MS (Fisons PQ2+ and Agilent 7500). Detection limits for REE were between 0.4 and 0.05 ppm for a 30 × 30 μm pit. Additional analyses of zircons from the Sesia–Lanzo Zone were carried out on a Perkin-Elmer ELAN 6000 ICP-MS with a 193-nm ArF Excimer laser at the Institut für Isotopengeologie und Mineralische Rohstoffe, ETH Zürich (Günther et al., 1997). Analytical conditions were similar to these reported by Schaltegger et al. (1999). Typical detection limits for a 40-μm pit were 0.02 ppm. Contamination from inclusions and/or different zones (core during a rim analysis and vice versa) was detected by monitoring several elements during LA-ICP-MS analysis and integrating only the 'clean' part of the signal. Analyses of the same crystal obtained by the two techniques are similar, even though a direct comparison is inappropriate because of the different volumes sampled (see also Hoskin, 1998).

3. Granulite-facies zircon (Reynolds Range)

The Reynolds Range, central Australia, consists of a Paleoproterozoic polymetamorphic basement with a sedimentary cover. The entire sequence was intruded by numerous granitic bodies producing local contact metamorphism before being regionally metamorphosed under low-pressure/high-temperature conditions in the early Mesoproterozoic. The regional event is well documented in both basement and cover (Clarke and Powell, 1991; Dirks et al., 1991; Vry et al., 1996; Buick et al., 1998), which preserve a metamorphic gradient from greenschist-to granulite-facies conditions (750–800 °C, 4.5–5 kbar). The age of the regional metamorphism is constrained by several SHRIMP U–Pb (Vry et al., 1996; Williams et al., 1996; Rubatto et al., 2001) and Pb–Pb (Buick et al., 1999) age determinations to the period 1560–1595 Ma. On the basis of field, petrographic and geochronological data, Rubatto et al. (2001) concluded that metamorphic zircon growth in the Reynolds Range occurred exclusively at granulite-facies conditions in the presence of partial melt.

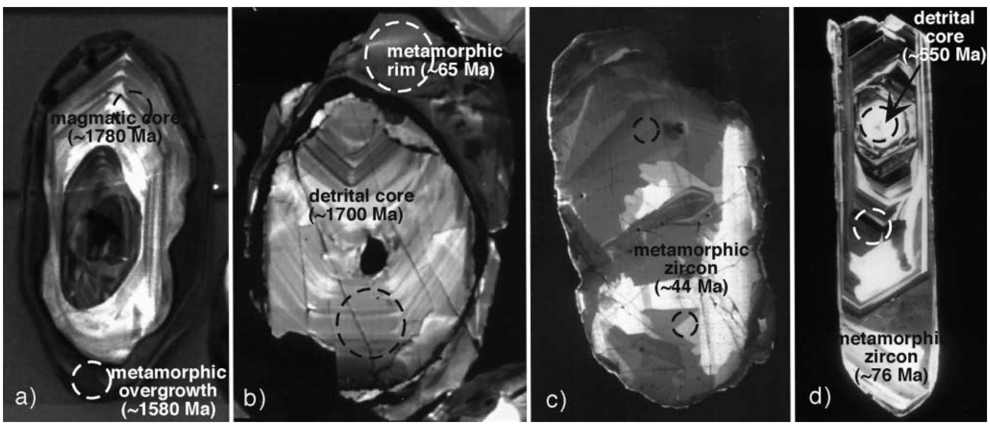

Fig. 1. Cathodoluminescence images of analysed zircon crystals. The circles indicate the location of the trace element analysis. (a) Zircon from garnet-bearing granulite GP7 (Reynolds Range) with a dark metamorphic rim surrounding a complex core. Spot 30 μm. (b) Zircon from eclogitic micaschist MST2a (Sesia–Lanzo Zone) with a metamorphic rim surrounding a detrital core. Spot 40 μm. (c) Zircon from eclogitic metasediment CIG3 (Zermatt–Saas Fee ophiolites), which formed during ultra-HP metamorphism. Spot 30 μm. (d) Zircon from metamorphic vein MST1 (Sesia–Lanzo Zone) with an oscillatory-zoned metamorphic rim on a bright detrital core. Spot 40 μm.

Table 1
Representative trace element analyses of zircon from granulite- and eclogite-facies rocks

Label	P	Ti	Y	Nb	La	Ce	Pr	Nd	Sm	Eu	Gd	Tb	Dy
Garnet-bearing granulites (Reynolds Range)													
GP7-1r	993	na	1275	0.87	0.348	1.18	0.100	1.37	1.06	0.185	9.73	5.92	104
average[a]	764		1108	0.948	0.356	1.91	0.167	1.05	1.42	0.219	11.7	6.17	95.0
stdev[a]	215		191	0.066	0.061	0.91	0.104	0.568	0.279	0.070	2.12	0.283	9.37
GL7-9r	922	na	1305	0.639	0.210	1.34	0.075	0.660	1.06	0.355	9.67	5.59	99.4
average[a]	861		1356	0.911	0.210	1.44	0.075	0.540	1.40	0.244	12.2	6.72	109
stdev[a]	55.2		98.4	0.236		0.151		0.196	0.367	0.097	2.59	1.08	11.5
GP7-6c	880	na	1687	0.551	0.330	3.26	0.181	1.79	3.65	0.307	26.1	10.7	147
GL7-6c	814	na	1552	0.335	0.121	2.02	0.115	1.66	3.64	0.158	25.7	10.2	140
average[a]	710		1411	0.541	0.325	2.95	0.167	1.96	3.94	0.295	25.1	9.75	129
stdev[a]	133		312	0.311	0.254	1.05	0.065	0.432	0.541	0.125	3.85	1.75	26.0
Garnet-free granulites (Reynolds Range)													
GP4-4r	742	na	1332	1.51	bd	3.16	0.106	0.486	bd	0.358	6.15	4.76	92.0
GP4B-12r	1104	na	1356	1.37	0.036	1.12	0.014	0.119	0.693	0.261	7.37	4.78	94.4
average[a]	1035		1425	1.31	0.075	2.30	0.060	0.481	1.06	0.365	8.53	5.36	101
stdev[a]	150		131	0.271	0.059	1.12	0.045	0.349	0.514	0.122	2.50	0.996	16.6
GL4B-26r	1720	na	2087	4.503	0.032	3.01	bd	0.337	1.42	0.462	12.9	8.55	159
average[a]	1502		2022	4.47	0.062	4.46	0.049	0.415	1.41	0.420	12.7	8.61	153
stdev[a]	286		261	0.27	0.065	1.74	0.037	0.175	0.329	0.169	3.08	1.95	32.0
GP4-4c	136	na	262	0.523	bd	9.22	0.078	0.339	1.63	0.129	4.50	1.61	24.1
GP4B-10c	1641	na	3397	1.03	bd	0.698	0.059	1.50	5.88	0.086	39.6	20.5	300
average[a]	609		1335	1.92	0.377	10.6	0.320	2.71	3.67	0.725	22.7	9.62	130
stdev[a]	557		1116	1.62	0.482	11.1	0.491	2.94	2.90	0.943	18.2	8.10	109
Eclogitic micaschist (Sesia–Lanzo Zone)													
MST2a-18r	na	na	32.9	na	bd	0.188	bd	0.015	0.030	0.133	1.55	0.439	3.11
MST2a-13r	46.4	1006	48.4	0.337	bd	0.169	bd	0.048	0.101	0.111	2.22	0.998	8.02
average[a]	54.6	902	57.6	0.300	bd	0.212	0.008	0.062	0.164	0.121	2.39	0.874	7.61
stdev[a]	11.4	91	24.0	0.036	bd	0.116	bd	0.032	0.095	0.058	1.22	0.436	3.64
MST2a-15c	na	na	208	na	bd	7.30	0.020	0.306	0.309	0.102	2.86	1.13	12.9
MST2a-19c	327	783	732	1.72	0.011	1.20	0.015	0.229	0.994	0.057	8.88	4.20	59.2
average[a]	251	807	453	2.28	0.014	10.2	0.033	0.579	1.04	0.232	6.52	2.46	32.7
stdev[a]	78.3	68.9	247	0.506	0.005	9.74	0.017	0.304	0.549	0.207	3.52	1.37	20.5
Metamorphic vein (Sesia–Lanzo Zone)													
MST1-5r	na	na	3251	na	0.019	9.01	0.019	0.641	1.27	0.594	16.4	9.14	166
MST1-10r	na	na	1132	na	bd	4.40	bd	0.259	0.455	0.227	5.18	3.02	55.6
MST1-29r	764	887	3746	29.7	0.027	15.8	0.024	0.303	1.90	0.810	24.7	14.2	254
average[a]	583	893	2682	22.0	0.116	10.3	0.053	0.470	1.23	0.532	14.7	8.34	149
stdev[a]	146	8	961	5.65	0.131	4.30	0.038	0.214	0.424	0.183	5.89	3.30	59.8
Ultra-HP eclogite and metasediments (Zermatt–Saas Fee ophiolites)													
CIG2-6	63.2	1664	46.9	0.149	bd	0.271	bd	bd	0.157	0.221	2.40	0.760	6.26
CIG2-4	44.5	1780	135	0.107	bd	0.177	bd	bd	0.206	0.312	3.40	1.30	13.8
average[a]	51.5	1782	69.1	0.127	bd	0.171	bd	bd	0.160	0.234	2.03	0.734	7.30
stdev[a]	8.13	186	43.9	0.017	bd	0.081	bd	bd	0.044	0.073	1.19	0.419	4.54
CIG3-11	264	1734	891	1.15	bd	2334	bd	bd	1.96	2.31	40.2	17.0	139
CIG3-9		1850	58.3	0.290	bd	0.223	bd	bd	bd	bd	0.834	0.416	5.17
average[a]	250	1545	448	1.64	bd	2183	bd	1.15	5.86	5.84	37.5	11.4	73.3
stdev[a]	144	401	471	1.816	bd	3495	bd	bd	6.90	6.25	56.0	13.8	89.1
CIG4-3	48.9	1779	1784	0.514	bd	265	bd	bd	0.268	0.389	11.1	8.93	150
average[a]	49.5	1635	1828	1.19	bd	381	bd	bd	0.490	0.977	17.6	10.4	151
stdev[a]	9.02	125	1286	0.694	bd	405	bd	bd	0.489	0.832	20.0	9.91	120

Ho	Er	Tm	Yb	Lu	Hf	Ta	Pb	Th	U	Th/U	Lu_n/Sm_n	Eu/Eu*
40.9	222	56.6	639	124	11,681	na	791	8.63	712	0.012	719	0.118
36.1	180	43.8	468	92.1	11,829		765	14.8	688	0.022	416	0.118
6.06	52.0	16.3	211	42.9	520		81.9	6.01	41.5	0.008	238	0.049
42.6	233	58.7	653	132	12,187	na	909	10.3	811	0.013	762	0.228
44.4	226	53.2	551	107	11,588		698	17.9	634	0.031	503	0.133
3.38	14.8	5.37	90.9	21.5	734		184	8.21	155	0.019	228	0.082
56.4	260	55.0	534	97.0	10,299	na	414	59.4	336	0.177	163	0.070
52.6	241	49.3	466	85.4	9736	na	287	67.3	210	0.320	144	0.037
48.3	217	45.1	427	78.1	9708		338	75.0	262	0.301	122	0.070
10.5	46.5	9.93	94.0	16.1	397		90.4	20.2	77.2	0.086	25.3	0.033
41.1	254	67.3	771	154	11,614	na	605	41.7	581	0.072		0.413
43.3	256	69.6	838	168	11,080	na	536	9.41	469	0.020	1483	0.223
46.9	278	77.0	856	176	11,256		487	18.0	441	0.039	1182	0.274
8.17	48.4	16.5	138	33.5	320		76.3	11.3	81.9	0.017	396	0.088
67.3	391	108	1272	257	11,878	na	1378	44.1	1135	0.039	1110	0.222
70.9	420	119	1299	274	11,584		1244	58.0	1020	0.058	1205	0.211
15.2	91.3	26.8	234	54.5	617		156	12.1	124	0.017	135	0.081
8.51	42.0	8.95	93.6	18.1	8718	na	159	49.1	98.2	0.500	67.8	0.137
113	538	110	1002	171	10,809	na	1363	124	954	0.130	178	0.013
49.7	231	47.5	455	88.1	10,159		2124	177	1248	0.227	180	0.246
41.8	187	35.3	307	56.4	1113		2577	136	1393	0.197	104	0.233
0.796	2.58	0.510	3.94	0.635	10,969	na	na	1.23	601	0.002	130	0.594
1.56	4.46	0.726	6.44	1.16	11,760	bd	1.11	1.36	250	0.005	70.2	0.336
1.63	5.35	0.902	7.60	1.38	11,004	0.088	0.627	1.37	349	0.005	67.9	0.401
0.762	2.59	0.369	3.27	0.643	593		0.487	0.520	166	0.002	35.7	0.115
4.96	24.4	6.11	64.2	12.4	10,778	na	na	48	698	0.068	246	0.221
23.7	124	28.5	281	58.6	10,632	1.52	2.21	29.8	619	0.048	361	0.040
13.0	67.2	15.5	157	32.5	10,659	1.60	9.39	78.1	845	0.164	206	0.223
8.21	43.7	9.93	97.1	20.8	1187	0.252	7.14	46.6	616	0.218	94.0	0.103
83.1	481	117	1208	261	14,550	na	na	183	6477	0.028	1260	0.234
28.2	171	42.1	441	101	15,982	na	na	62.4	2858	0.022	1352	0.279
121	717	177	1777	354	10,981	887	2.26	275	3157	0.087	1143	0.211
73.2	434	107	1084	229	12,234	893	2.05	163	4300	0.046	1229	0.224
28.3	166	41.6	415	81.4	2635	7.95	1.38	80.8	2707	0.025	158	0.031
1.46	4.79	0.802	7.38	1.41	8306	bd	bd	2.66	316	0.008	54.6	0.602
4.13	15.6	2.80	24.1	4.43	9024	bd	bd	1.99	192	0.010	132	0.603
2.11	7.98	1.52	13.9	2.65	8864		4.10	1.62	204	0.008	93.9	0.459
1.36	5.09	0.888	7.43	1.35	732			0.918	94.9	0.002	38.6	0.307
25.4	60.4	7.21	42.1	5.41	9316	0.410	bd	5.12	7.99	0.640	16.9	0.383
1.65	6.11	1.06	7.77	1.26	11,349	0.113	bd	0.859	95.7	0.009		
13.2	31.9	3.85	22.4	2.93	9705	0.468	0.759	21.7	56.9	0.683	9.73	0.222
14.3	29.8	3.092	15.9	1.81	1611	0.475		51.7	78.6	1.37	7.29	0.253
53.6	218	37.6	341	54.5	9121	0.123	bd	2.88	2.45	1.17	1245	0.241
53.8	226	39.0	349	55.6	8735	0.198		4.67	6.73	0.902	964	0.170
37.3	142	22.5	162	27.4	481	0.093		1.95	4.82	0.464	416	0.148

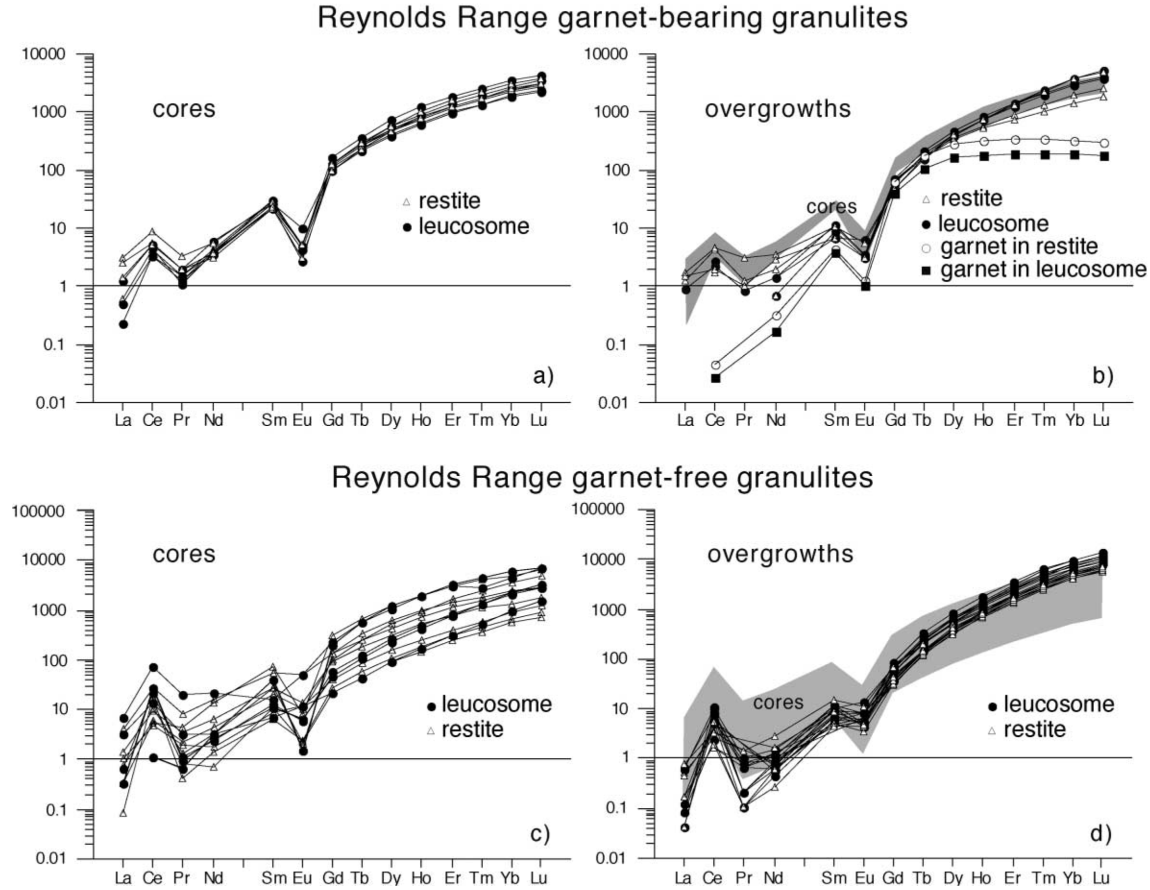

Fig. 2. Chondrite normalised REE patterns of zircon cores and metamorphic overgrowths from garnet-bearing (a and b) and garnet-free (c and d) granulites of the Reynolds Range. The average composition of garnet coexisting with metamorphic zircon is reported in (b). 1σ errors for the MREE and HREE in garnet are comparable to the size of the symbols. Normalisation after Sun and McDonough (1989).

3.1. Garnet-bearing metagranite

Several granitic bodies that intruded the Reynolds Range sequence recorded HT metamorphism and anatexis, which developed the paragenesis garnet + biotite + cordierite + K-feldspar ± plagioclase + monazite + zircon. Zircons in restitic granulite GP7 and leucosome GL7 have rims formed during the Proterozoic metamorphic event as overgrowth on cores of magmatic origin (Fig. 1a; Rubatto et al., 2001). Because the cores analysed are mainly inherited from the granitic protolith, their trace element composition (Table 1, Fig. 2a) is much more uniform than is normally observed for detrital cores (see below). These magmatic cores have medium Th (55–110 ppm) and U contents (152–336 ppm) with a typically magmatic Th/U ratio of 0.18–0.47. They contain approximately 1–1.4 wt.% of HfO_2, between 1000 and 2000 ppm of Y, a small amount of Nb (0.21–1.3 ppm, av. 0.54 ppm) and a moderate amount

Notes to Table 1:
r = Rim; c = core; na = not analysed; bd = below detection; Lu_n/Sm_n = normalised to chondrite after Sun and McDonough (1989).
[a] Average and standard deviation values for each zircon category are based on a larger number of analyses (see Background Data Set, http://www.elsevier.com/locate/chemgeo).

of P (522–880 ppm) to charge-compensate the uptake of Y^{+3} and REE^{+3}. The oscillatory zoning present in all the crystals is, at least in part, responsible for compositional variations among grains and within single grains. The chondrite normalised REE pattern for these zircons (Fig. 2a) is enriched in HREE ($Lu_n/Sm_n = 92–163$, av. 122), has a positive Ce anomaly and a negative Eu anomaly (Eu/Eu* = 0.04–0.15, av. 0.07), as is commonly observed in magmatic zircon (Hinton and Upton, 1991; Paterson et al., 1992; Hoskin, 1998; Cornell et al., 1999; Hoskin and Black, 2000; Hoskin and Ireland, 2000).

The metamorphic zircon overgrowths from both restite and leucosome (Table 1) are not zoned and therefore have more uniform composition. They differ from the cores in having lower Th contents (8.6–27 ppm), higher U contents (520–811 ppm) and hence lower Th/U ratios (0.01–0.05). They are slightly richer in Nb (0.64–1.0 ppm, av. 0.93 ppm) than the cores, but have similar Y and P contents. Their Hf content is rather constant (1.3–1.4 wt.% HfO_2). The REE patterns of the metamorphic overgrowths (Fig. 2b) are steeper ($Lu_n/Sm_n = 208–719$, av. 454) than those of the cores, mainly because of the decrease in MREE concentrations. They have similar negative Eu anomalies (Eu/Eu* = 0.08–0.23, av. 0.12) and positive Ce anomalies. There is no significant difference in zircon overgrowth composition between restite and leucosome, suggesting that trace element equilibrium between restite and melt was achieved (Rubatto et al., 2001).

3.2. Garnet-absent metapelites

The Reynolds Range metapelites have a peak paragenesis consisting of cordierite, biotite, sillimanite, K-feldspar, quartz, magnetite, monazite and zircon. Zircon crystals in both restitic metapelite (GP4 and GP4B) and melt segregates (GL4B) have metamorphic overgrowths on detrital cores of mainly magmatic origin (see Rubatto et al., 2001).

The detrital cores have a range of trace element compositions, as expected for grains derived from different sources (Table 1 and Fig. 2c). Most of the cores have Th/U ratios of 0.1–0.7, which is consistent with a magmatic origin (Williams et al., 1996; Rubatto and Gebauer, 2000). The cores are typically enriched in HREE ($Lu_n/Sm_n = 53–426$), have a positive Ce anomaly and a negative Eu anomaly (Eu/Eu* = 0.84–0.01). The metamorphic zircon overgrowths from both restite and leucosome are similar to those found in the garnet-bearing granulite (Table 1 and Fig. 2d) with typically low Th/U ratios (0.07–0.02). The main difference with respect to the garnet granulite is a slightly higher REE content and a stronger enrichment in HREE ($Lu_n/Sm_n = 463–1514$, av. 1193).

4. Eclogite-facies zircon (Sesia–Lanzo Zone and Zermatt–Saas Fee ophiolites)

The Sesia–Lanzo Zone is the largest unit of eclogite-facies crustal material in the Alps. It consists mainly of a polymetamorphic basement intruded by pre-Alpine granitoids and mafic bodies (Compagnoni, 1977). Eclogite-facies assemblages within the Sesia–Lanzo Zone are preserved mainly in the Eclogitic Micaschist Complex (Compagnoni, 1977) for which peak metamorphic conditions of 15–18 kbar and 550–620 °C have been estimated (Compagnoni, 1977; Pognante, 1989). The age of Alpine high-pressure (HP) metamorphism in this unit has been constrained at ~65 Ma by several geochronological studies (Ramsbotham et al., 1994; Inger et al., 1996; Dûchene et al., 1997), including zircon dating (Rubatto et al., 1999).

The Zermatt–Saas Fee ophiolites tectonically overlie the Sesia–Lanzo Zone. They consist of ultramafic, mafic and sedimentary rocks (Bearth, 1967) that underwent eclogite-facies metamorphism during the Alpine orogeny (Barnicoat and Fry, 1986). The samples investigated are from Lago di Cignana, a locality were ultra-HP conditions have been documented (28–30 kbar and ~600 °C; Reinecke, 1991). The age of metamorphism in this locality has been constrained at 44.1 ± 0.7 Ma by SHRIMP U–Pb zircon dating (Rubatto et al., 1998).

4.1. Eclogite-facies metasediments and eclogite

Eclogite-facies metasediments of the Eclogitic Micaschist Complex (Sesia–Lanzo Zone) mainly consist of garnet, omphacite, phengite, Na amphibole and quartz, with secondary albite and chlorite. Zircon from one metasediment (MST2a; Fig. 1b) preserves detrital cores (apparent ages between 390 and 2464 Ma; Rubatto et al., 1999) surrounded by metamorphic rims. The zircon rims formed by recrystallisation of pre-existing detrital zircon and, unlike the case of the granulites, do not represent new growth during metamorphism. In fact, some of the rims yielded mixed ages between the age of core and that of HP metamorphism (65 ± 3 Ma; Rubatto et al., 1999) indicating that U–Pb resetting by recrystallisation was not always complete.

Trace element analyses of zircon cores and rims revealed significant differences in composition between the two domains (Table 1). Similarly to the metapelitic granulites, the detrital cores are characterised by a wide range of trace element compositions. They have medium to high Th (28–139 ppm) and U contents (216–2095 ppm) with a Th/U ratio in the range 0.03–0.6, and medium Y, Ti, P and Nb contents. In general, the chondrite normalised REE patterns (Fig. 3a) are enriched in HREE (Lu_n/Sm_n = 76–361, av. 206), have positive a Ce anomaly and a negative Eu anomaly (Eu/Eu* = 0.04–0.36, av. 0.22).

The metamorphic ‘s have a distinctive chemical composition characterised by low Th/U ratios (< 0.01) and much lower Th, U, Y, Nb, P and REE concentrations. They are less enriched in HREE (Lu_n/Sm_n = 39–130, av. 68) than the zircon cores and a have smaller negative Eu anomaly (Eu/Eu* = 0.32–0.59, av. 0.40). These data support the conclusion of

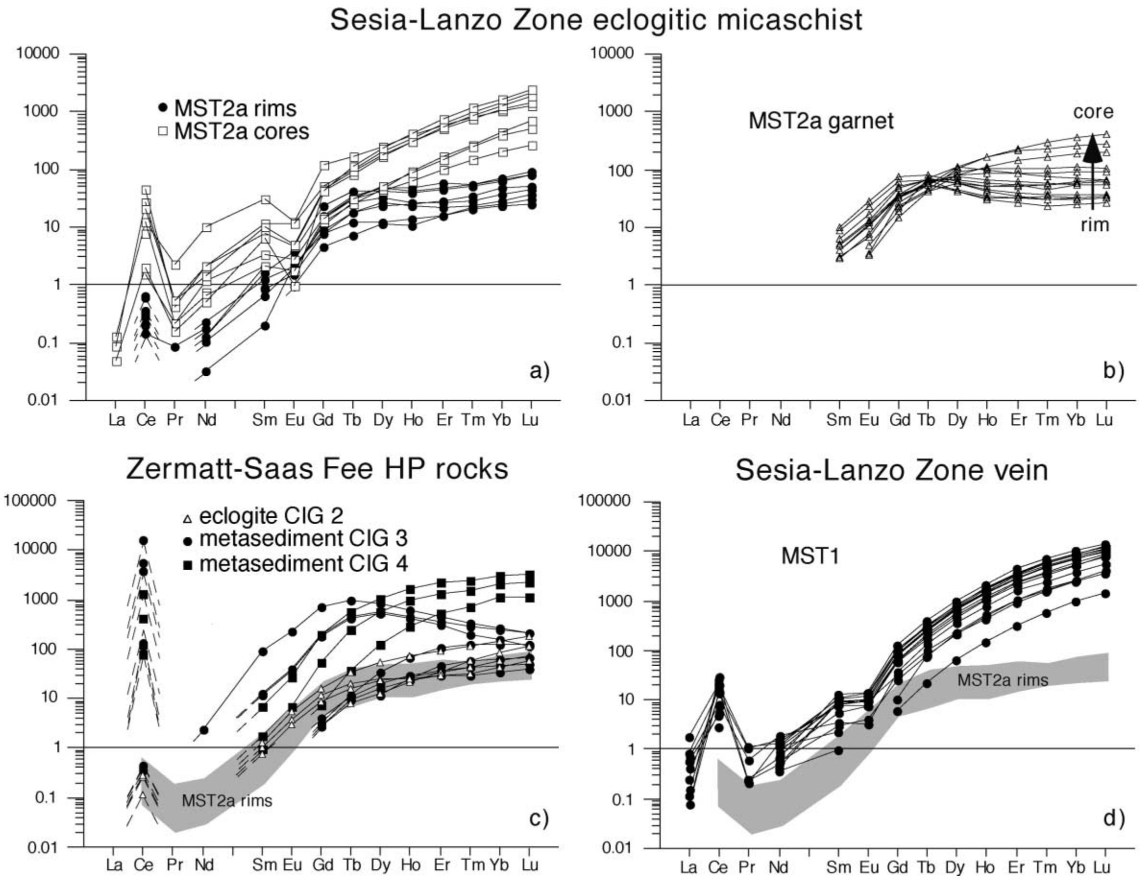

Fig. 3. Chondrite normalised REE patterns of (a) zircon cores and metamorphic rims from eclogitic micaschist MST2a (Sesia–Lanzo Zone); (b) garnet from eclogitic micaschist MST2a; (c) metamorphic zircon from Lago di Cignana eclogitic rocks (Zermatt–Saas Fee ophiolites); (d) metamorphic vein MST1 from the Sesia–Lanzo Zone. Normalisation after Sun and McDonough (1989).

Hoskin and Black (2000) that HREE are expelled from zircon during sub-solidus recrystallisation.

Metamorphic zircon was found in one eclogite (CIG2, garnet + omphacite + Na amphibole + phengite + rutile) and two Mn-rich metasediments (CIG3 and CIG4, quartz + garnet + phengite ± epidote ± rurutile ± ankerite) from the Zermatt–Saas Fee ophiolite. It is present either as rims around pre-existing detrital cores (only in metasediments) or as fully metamorphic crystals characterised by sector zoning (Fig. 1c; see also Rubatto et al., 1998). Because of the low metamorphic temperature and the zoning pattern, zircons in these eclogitic rocks are believed to have formed under sub-solidus conditions, possibly in the presence of fluids (Rubatto et al., 1998).

Zircon from the eclogite CIG2 is similar in composition to zircon rims in the eclogitic micaschists MST2a. The metasediment zircons have similarly low Th/U ratios and Nb contents, but their trace element content is more variable and often much higher (Table 1). However, despite differences in trace element content, which are most probably caused by differences in host rock composition, metamorphic zircon in both eclogite and metasediments have a small negative Eu anomaly (Eu/Eu* = 0.24–0.63) and a chondrite-normalised pattern that lacks the typical enrichment in HREE of magmatic or HT zircon (Fig. 3c). In fact, even in zircons rich in MREE, the HREE show only a small enrichment or even a depletion with respect to MREE, which produces an unusual REE pattern with negative slope. Zircons from the metasediments appear to have an extreme Ce positive anomaly.

4.2. Metamorphic vein

The eclogitic micaschist of the Sesia–Lanzo Zone hosts a series of metamorphic veins, which preserve an eclogite-facies mineral assemblage. A quartz–omphacite–phengite vein contains euhedral, oscillatory-zoned zircons that rarely preserve detrital cores (Fig. 1d; apparent ages 309–532 Ma; Rubatto et al., 1999). The age of these zircons (76 ± 1 Ma; Rubatto et al., 1999) is significantly older than the age of metamorphic zircon rims in the country rock micaschist (65 ± 3 Ma; Rubatto et al., 1999), an unexpected result as both vein and country rock have eclogite-facies paragenesis. To explain the apparent paradox, Rubatto et al. (1999) suggested that the vein and its zircon precipitated from fluids during prograde metamorphism, and that the metamorphic zircon in the country rock formed later at the metamorphic peak.

Like the metamorphic zircon rims in the surrounding micaschist, the zircons in the vein have a low Th/U ratio, but they are characterised by much higher trace element contents, especially Y (1132–4249), Nb (14–30) and HREE, which are not compensated by P uptake (Table 1). Their REE pattern is also distinct from the metamorphic zircon in the country rock micaschist (Fig. 3d). The zircons in the vein have a much steeper REE pattern (Lu_n/Sm_n = 1001–1576, av. 1229) and a marked negative Eu anomaly (Eu/Eu* = 0.15–0.28, av. 0.22). Detrital cores from this sample were too small to obtain clean trace element analyses, however their age and Th–U composition is similar to the zircon cores found in the country rock micaschist (Rubatto et al., 1999).

5. Discussion

5.1. Metamorphic zircon composition

Several previous studies (Murali et al., 1983; Heaman et al., 1990; Hinton and Upton, 1991; Maas et al., 1992; Paterson et al., 1992; Barbey et al., 1995; Peucat et al., 1995; Schaltegger et al., 1999; Hoskin and Black, 2000; Hoskin and Ireland, 2000) have documented the preference of zircon for Hf, Y and the HREE over the LREE, and the presence in terrestrial zircon of a positive Ce anomaly and a negative Eu anomaly. Zircon/melt partition coefficients obtained experimentally (Watson, 1980) and from natural systems (Nagasawa, 1970; Murali et al., 1983; Fujimaki, 1986; Hinton and Upton, 1991) vary over an order of magnitude but generally confirm zircon's preference for the HREE. The metamorphic zircon investigated here is similar to magmatic zircon in terms of its high Hf and Y contents, positive Ce anomaly and enrichment in HREE with respect to LREE. However, metamorphic zircon has some particular features that distinguish it from magmatic zircon.

Despite several differences, metamorphic zircons that formed in different environments share some

Table 2
REE composition of garnet in restitic granulite GP7 and coexisting leucosome GL7

	GP7 restite		GL7 leucosome	
	Av. $n=12$	$\pm 1\sigma$	Av. $n=12$	$\pm 1\sigma$
La	bd	bd	bd	bd
Ce	0.028	0.006	0.016	0.014
Pr	bd	bd	bd	bd
Nd	0.15	0.04	0.077	0.068
Sm	0.66	0.24	0.58	0.21
Eu	0.073	0.014	0.060	0.011
Gd	12.4	1.4	7.9	0.8
Tb	6.6	0.3	3.8	0.6
Dy	71.7	3.8	41.5	7.5
Ho	18.0	1.1	10.3	1.8
Er	56.5	3.2	32.0	5.5
Tm	8.4	0.5	4.8	0.8
Yb	54.6	3.5	31.7	5.9
Lu	7.6	0.5	4.5	1.0

bd = Below detection

similarities in trace element compositions. As previously reported, metamorphic zircon typically has a low Th/U ratio, which in some cases is, together with its distinctive cathodoluminescence zoning, the major distinguishing feature between metamorphic and magmatic zircon. The enrichment in HREE with respect to LREE is much more variable than that observed in magmatic zircon (e.g., Hoskin and Ireland, 2000). The pronounced negative Eu anomaly observed in magmatic zircon (with the exclusion of kimberlitic zircon; Belusova et al., 1998) is found also in metamorphic zircon formed in the presence of melt, but is significantly reduced in lower temperature zircon.

The variety of compositions and REE patterns observed in zircon from the two different metamorphic settings (granulite and eclogite facies) is a clear indication that, in metamorphic environments, zircon chemistry is subject to drastic changes. This is different from magmatic zircon, which shows limited chemical variation among Si-rich rocks, an observation that led Hoskin and Ireland (2000) to discount the possibility of using zircon trace element composition as a provenance indicator. In contrast, metamorphic zircon is likely to bear information on the conditions of its formation. In order to understand this information, the most distinctive features of metamorphic zircon need to be analysed in detail in the light of the zircon-forming processes.

5.2. Zircon–garnet coexistence

Garnet is the most important mineral for thermobarometry, whereas zircon is one of the best geochronometers. As a consequence, if coexistence between these two minerals can be proved it would be possible to link U–Pb ages to metamorphic conditions and thus obtain detailed P–T–time paths. Garnet and zircon are uniquely suited for this exercise because both minerals are enriched in Y and HREE. Therefore, when coexisting, zircon and garnet will influence each other's compositions.

Garnet formed in the granulitic migmatites of the Reynolds Range as a solid phase during the melting reaction biotite + sillimanite + quartz = garnet + cordierite + melt. Rubatto et al. (2001) demonstrated that metamorphic zircon overgrowths in the Reynolds Range formed in the presence of melt and therefore coexisted and were in equilibrium with garnet. With the exception of a small retrograde rim, garnet in both restite and leucosome is not zoned and has a uniform Ca and Fe/Mg composition as well as

Table 3
Trace element partition coefficients between zircon and garnet

	GP7[a]	GL7[a]	MST2a[b]	MST2a[b]
	Gt av.	Gt av.	Gt rim	Gt core
Ti	nc	nc	8.3	4.2
Y	2.3	4.8	1.3	0.22
Nb	12	nc	21	5.4
La	nc	nc	nc	nc
Ce	69	90	nc	nc
Pr	nc	nc	nc	nc
Nd	7.0	5.7	0.60	nc
Sm	2.1	2.4	0.27	nc
Eu	3.2	4.0	0.19	nc
Gd	0.94	1.6	0.34	0.35
Tb	0.93	1.8	0.44	0.42
Dy	1.3	2.6	0.70	0.26
Ho	2.0	4.3	0.97	0.17
Er	3.2	7.1	1.2	0.13
Tm	5.2	11	1.5	0.12
Yb	8.6	17	1.8	0.12
Lu	12.1	23.9	2.1	0.13
Hf	24085	48452	nc	170739

nc = Not calculated because the element was not measured or not detectable in either one or both minerals.

[a] Equilibrium partitioning calculated using an average composition for metamorphic zircon and garnet in each sample.

[b] Partitioning calculated from average zircon rim composition and the two extreme garnet compositions from Fig. 3b.

constant REE contents (Table 2 and Fig. 2b). This provides evidence that garnet reached equilibrium with the melt in both major and trace elements. This is confirmed by the fact that the REE composition of garnet in restite and leucosome is remarkably similar. The identical isotopic and chemical compositions of the zircon overgrowths in restite and leucosome also argue that equilibrium between zircon and melt was reached in both samples (see also Rubatto et al., 2001).

The equilibrium between garnet-melt and zircon-melt in leucosome and restite allows the calculation of zircon/garnet trace element partition coefficients (${}^{TE}D_{zir/gt}$; Table 3 and Fig. 4). The ${}^{TE}D_{zir/gt}$ in both rock types show that Y, Nb and particularly Hf are preferentially hosted in zircon. Among the REE, the HREE, Ce, Sm, Nd and Eu are enriched in zircon with the MREE being almost equally distributed between both minerals. The slight difference in ${}^{TE}D_{zir/gt}$ between the two samples is mainly due to the small variation in garnet composition. This variation is insignificant however when compared to the wide range of ${}^{REE}D_{zir/gt}$ obtained through the calculated ${}^{REE}D_{zir/melt}$ of Hinton and Upton (1991) and various ${}^{REE}D_{gt/melt}$ determined by analysing garnet megacrysts and ground mass in dacites and rhyolites (Fig. 4; Schnetzler and Philpotts, 1970; Irvin and Frey, 1978; Sisson and Bacon, 1992). The variation in ${}^{REE}D_{zir/gt}$ obtained from the literature would be even bigger if different ${}^{REE}D_{zir/melt}$ are used, which vary over an order of magnitude (Nagasawa, 1970; Watson, 1980; Murali et al., 1983; Fujimaki, 1986; Hinton and Upton, 1991).

This is the first report of zircon–garnet partitioning in metamorphic rocks where garnet and zircon can be proved to be in equilibrium. This partitioning is of great importance not only to establish if zircon and garnet are in equilibrium, but also to determine at what stage zircon formed in metamorphic rocks where the garnet is zoned, as shown in the following example.

In eclogitic micaschist MST2a, the garnet decreases in Ca content and increases in MgO/(MgO + FeO_{tot}) from core to rim (Fig. 5). This zoning in major elements suggests that the garnet grew during prograde metamorphism and that the Mg-rich rim represents peak conditions. Strong zoning is also observed in trace elements, with a drastic decrease in Ti, Y and HREE from core to rim (Fig. 3b). The amount of metamorphic zircon in this rock is very limited (a few

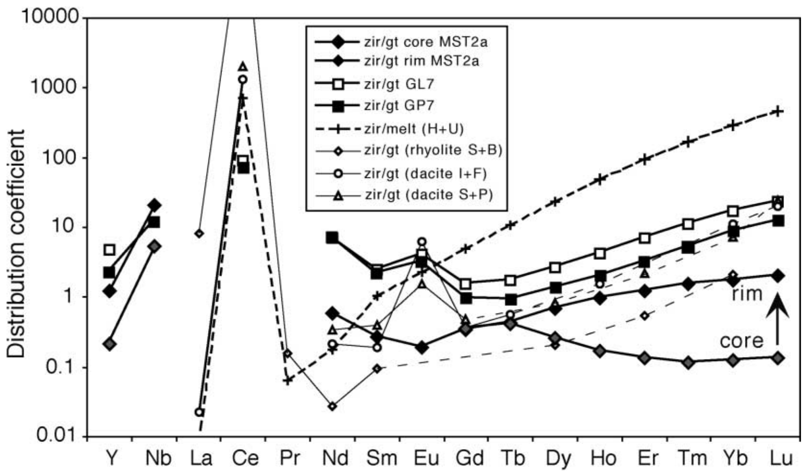

Fig. 4. Trace elements partition coefficient between zircon and coexisting garnet or melt. Values for GP7 and GL7 are calculated using an average composition for metamorphic zircon and garnet in each sample. For eclogite-facies micaschist MST2a, the distribution coefficients are calculated from average zircon rim composition and the two extreme garnet compositions from Fig. 3b. Zircon/melt values are from Hinton and Upton (1991). Zircon/garnet partitioning is obtained via zircon/melt values (Hinton and Upton, 1991) and garnet/melt data from Sisson and Bacon (1992), Irvin and Frey (1978) and Schnetzler and Philpotts (1970). These authors obtained garnet/melt data by analysing garnet megacrysts and the ground mass, which was assumed to resemble the melt composition. See text for discussion.

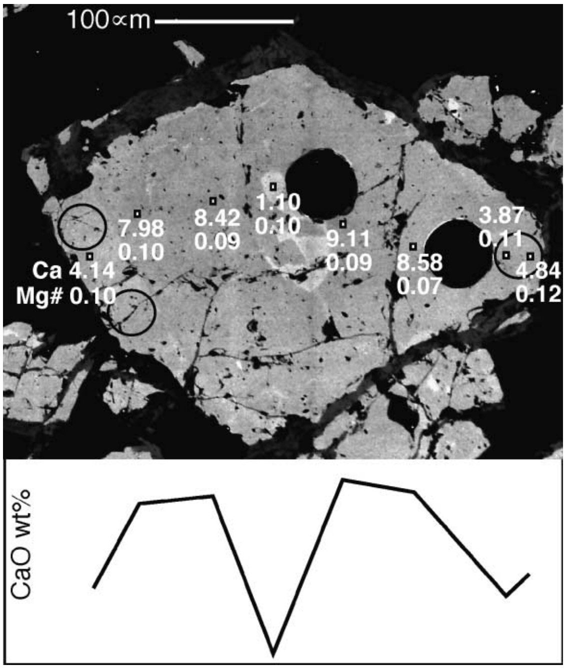

Fig. 5. Backscattered electron (BSE) image of garnet from eclogitic micaschist MST2a. Electron microprobe analyses were performed across the garnet and the relative wt.% of CaO and the Mg# = MgO/($MgO + FeO_{tot}$) are reported. The Ca content is also plotted at the base of the image. The high BSE–low Ca core is probably a relict of pre-Alpine metamorphism. Black and empty circles represent LA-ICP-MS analysis pits.

30–50 μm rims), and therefore at any given time, the ratio between the amount of garnet (10–15% of the rock) and the amount of zircon forming was ≫100. Assuming $^{TE}D_{zir/gt}$ similar to that observed in the Reynolds Range granulites, it is to be expected that the zircon chemical composition would be controlled by garnet formation. This predicts the HREE depletion documented in the metamorphic zircon rims, which recrystallised in the presence of garnet. When $^{TE}D_{zir/gt}$ are calculated using the different garnet compositions the resulting patterns also show a rotation (Fig. 4). Only the $^{TE}D_{zir/gt}$ values calculated from the garnet rim composition resemble in trend and absolute values the distribution coefficients obtained from the migmatitic granulites. This demonstrates that the metamorphic zircon rims formed in equilibrium with the Mg-rich garnet rim and hence that zircon recrystallisation in the eclogitic micaschists occurred at the HP peak. An implications of this is that the detrital zircon cores in sample MST2a, which do not show depletion in HREE, grew in the absence of garnet or any other HREE-rich phase. This is in line with their magmatic zoning, which suggests that they grew in a magmatic, possibly granitic magma where garnet is generally absent.

The difference between the $^{TE}D_{zir/gt}$ values obtained from the eclogites and the granulites has two possible explanations. The strong zoning of the eclogitic garnet might be on a smaller scale than the 30 μm of the laser analyses, preventing accurate measurement of the composition of the HP garnet rim. Alternatively, the $^{TE}D_{zir/gt}$ may vary with pressure and/or temperature, a possibility that is currently under investigation using natural and experimental data.

5.3. Open vs. closed system

Garnet in the granulite-facies rocks of the Reynolds Range is unzoned, and metamorphic zircon rims in garnet-bearing and garnet-free rocks are similar in HREE composition. These observations suggest that, in leucosome and restite of both rock types, garnet and zircon formed in an ‘open’ system situation with an infinite reservoir of trace elements, namely the melt. This prevented any change in zircon composition due to the crystallisation of garnet or other minerals.

On the other hand, the reduction in trace elements with ongoing metamorphism documented in the garnet from the eclogitic micaschist MST2a suggests garnet growth in a ‘closed’ system. This implies a limited reservoir of trace elements (the reactive portion of the bulk rock) that was progressively depleted by the growth of garnet, the only mineral in these rocks that contains significant amount of HREE. This prograde depletion in HREE translates to a rotation of the chondrite-normalised REE patterns of garnet itself (Fig. 3b), which in turn has influence on the chemistry of zircon formed in equilibrium with garnet. In fact, in this and other eclogite-facies rocks (CIG2, CIG3 and CIG4), metamorphic zircon is characterised by a flat HREE pattern, which occasionally can have even a negative slope (Fig. 3c). As metamorphic zircon growth in these eclogite-facies rocks occurred under sub-solidus conditions in the absence of any melt, the attribution of ‘closed’ system is realistic. Similar patterns have been reported for zircon in garnet-bearing granulites (Schaltegger et al., 1999) and HT eclogites (Hermann et al., 2001).

Similarly, in other rocks where zircon formed in a 'closed' system, the formation of REE-rich minerals such as monazite (for LREE and MREE), titanite (for LREE and MREE) or feldspars (for Eu) can potentially be recorded in the zircon composition.

5.4. Negative Eu anomaly and presence of feldspars

A negative Eu anomaly is a common feature of zircon in granitic rocks sensu lato (e.g., Murali et al., 1983; Hinton and Upton, 1991; Paterson et al., 1992; Hoskin and Ireland, 2000) and HT metamorphic rocks (Schaltegger et al., 1999; Hoskin and Black, 2000; Rubatto et al., 2001). It has been suggested that the negative Eu anomaly in zircon is either due to its coexistence with K-feldspar (Murali et al., 1983; Hinton and Upton, 1991), a known sink for Eu, or to Eu depletion of the rock as a whole (Schaltegger et al., 1999).

A marked negative Eu anomaly is observed in most of the samples investigated here: the magmatic zircon cores and metamorphic overgrowths in the Reynolds Range granulite, the detrital zircon cores in the eclogitic micaschist and the zircon from the metamorphic vein in the Sesia–Lanzo Zone. Both the magmatic inherited cores and the metamorphic overgrowths in the Reynolds Range samples formed in the presence of partial melt which crystallised as K-feldspar + quartz ± plagioclase. The negative Eu anomaly in zircon could either be inherited from the protolith or be the product of concurrent crystallisation of the melt to form feldspar. Unfortunately, the absence of metamorphic zircon growth in the lower temperature section of the Reynolds Range, where melt is absent, does not allow testing of the above hypotheses.

The negative Eu anomaly is consistently smaller in zircon from eclogite-facies samples than in any HT or magmatic zircon (Fig. 3a and c). The small Eu anomaly is independent of the rock type and appears to be a feature characteristic of metamorphic zircon in eclogitic rocks. The apparent decrease in Eu anomaly in these zircons is in line with the fact that the rocks never underwent partial melting (metamorphic peak temperatures were ≤ 600 °C in both localities). It is also an indication that zircon did not compete with feldspar for Eu, otherwise a much bigger anomaly would be present. This implies that zircon recrystallisation in these samples occurred in a feldspar-free paragenesis, and further supports the hypothesis of zircon formation at eclogite-facies conditions where feldspars were unstable. In fact, at any time during the prograde or retrograde path (blueschist and greenschist facies) albite was stable and it broke down to form jadeite + quartz only at eclogite-facies conditions. The small Eu anomaly that is present in the eclogite-facies zircon from both localities ($Eu/Eu^* = 0.24–0.63$) is most likely inherited from the whole rock composition, a suggested by Hermann et al. (2001) in HT eclogites. Moreover, reducing conditions (i.e., high Eu^{2+}/Eu^{3+}) are to be expected during HP metamorphism of sediments.

Zircon in the quartz–omphacite–phengite vein MST1 shows a bigger Eu anomaly ($Eu/Eu^* = 0.15–0.28$, av. 0.22) than the eclogite-facies zircon in the metasediment. This could indicate that the vein zircon formed when plagioclase or K-feldspar was stable, i.e. before eclogite-facies conditions. It is extremely unlikely that the negative Eu anomaly in these zircons is due to highly reducing conditions where only Eu^{2+}, which is not expected to enter zircon, is present, particularly because in the country rock micaschist metamorphic zircon has no negative Eu anomaly. Zircon formation in the vein at low grade is in line with the hypothesis of Rubatto et al. (1999), who, on the base of U–Pb ages, concluded that these zircons formed in the vein during prograde greenschist-facies metamorphism, under conditions where albite was stable. Zircon growth at similarly low temperatures has also been documented Liati and Gebauer (1999). The strong enrichment in HREE of these zircons is consistent with the absence of garnet in the vein. The high HREE and trace element contents in these zircons are unusual even for magmatic zircon and most likely reflects the composition of the metamorphic fluid. Alternatively, higher ${}^{TE}D_{zir/fluid}$ than in melt could be responsible for trace element enrichment in such hydrothermal zircon.

5.5. Depletion in mree in metamorphic zircon

The metamorphic zircon overgrowths in the Reynolds Range granulites have a steeper REE pattern than the magmatic or detrital cores (Fig. 2b and d), mainly due to lower MREE contents rather than to HREE enrichment. Similar patterns have previously been observed in zircon rims from HT gneisses (Peucat et al., 1995; Hoskin and Black, 2000). Hoskin and Black (2000) interpreted this feature as due to preferential expulsion of larger ions (LREE) during the sub-solidus recrystallisation of the zircon rims. However, this explanation is not applicable to the Reynolds Range, in which metamorphic zircon formed by new growth from a melt (Rubatto et al., 2001). An alternative explanation was proposed by Peucat et al. (1995) who suggested that the depletion in MREE in metamorphic zircon be caused by the concurrent growth of monazite, a phase rich in LREE and MREE. However, as previously argued, the garnet and zircon compositions indicate that metamorphic zircon crystallisation occurred in an 'open' system with a virtually infinite reservoir of trace elements. In such an environment it is unlikely that concurrent monazite growth could affect zircon composition.

The most likely explanation for the reduction in MREE content in the HT metamorphic zircon is therefore a partial melt depleted in MREE when compared to granitic compositions. A slight difference in melt composition would also explain the difference in HREE pattern between zircon overgrowths in the metagranite and the metapelite. This also implies that the concurrent growth of monazite cannot explain the low Th/U of the metamorphic zircon overgrowths from the granulites. The low Th/U in metamorphic zircon could be caused by one of the mechanism discussed by Rubatto and Gebauer (2000) or by a very low ${}^{Th}D_{zir/partial\ melt}$.

6. Conclusions

Zircon trace element composition can assist in distinguishing magmatic from metamorphic zircon, particularly metamorphic zircon formed at eclogite-facies conditions. Moreover, zircon composition is a powerful tool to identify equilibrium between metamorphic zircon and major minerals, which are indicative of specific metamorphic conditions.

Zircon trace element composition varies significantly according to formation process (crystallisation vs. recrystallisation) and fluid/melt involved. Zircon overgrowths crystallised during HT metamorphism in equilibrium with partial melt have compositions similar to magmatic zircon; they are rich in U, Y, Hf and P, have steep REE patterns ($Lu_n/Sm_n \sim 200-1500$) with positive Ce anomalies and negative Eu anomalies (Eu/Eu* 0.08–0.41). Their low Th/U ratio (< 0.07) is the only chemical feature that distinguishes them from magmatic zircon. The REE composition of garnet and metamorphic zircon in the Reynolds Range granulites indicate equilibrium between these two minerals and permits, for the first time, the direct calculation of ${}^{TE}D_{zir/gt}$. The partitioning is highly in favour of zircon for Hf and between ~ 1 and 90 for Y, Nb and the REE with a maximum for Ce and HREE and a minimum for MREE. The low MREE content of HT metamorphic zircon with respect to magmatic zircon cannot be attributed to crystallisation of monazite, and is most likely due to MREE depleted in the partial melt.

At eclogite-facies conditions, sub-solidus zircon growth occurs in a 'closed' system with limited supply of trace elements, i.e. the reactive bulk. This induces changes in zircon composition according to the coexisting mineral assemblage. Sub-solidus garnet formation produces depletion in HREE in the reactive bulk, which results in the HREE patterns of the coexisting metamorphic zircon being nearly flat or with a negative slope. Through the composition of metamorphic zircon and the equilibrium ${}^{TE}D_{zir/gt}$ values, it is possible to identify the specific zone in garnet that formed in equilibrium with the zircon. This correlation provides a direct link between datable zircon domains and pressure–temperature conditions that can be obtained from garnet. Zircon that formed in a feldspar-free assemblage does not compete with feldspars for Eu and it will therefore have a reduced negative Eu anomaly with respect to magmatic and HT metamorphic zircon. Therefore, eclogite-facies zircon is characterised by flat HREE pattern and small Eu anomaly.

Acknowledgements

I am grateful to Detlef Günther (ETH) and Charlotte Allen (RSES) for technical support in LA-ICP-MS REE analysis and data reduction. Ian S. Williams helped with SHRIMP analysis. I thank Jörg

Hermann for constructive discussion and review of the manuscript. Comments from M. Palin, I.S. Williams, T. Ireland, D. Cherniak, P. Barbey and R.W. Hinton, and the journal reviews from G. Fraser and J.M. Mattinson are gratefully acknowledged. **MB**

References

Barbey, P., Allé, P., Brouand, M., Albarède, F., 1995. Rare-earth patterns in zircons from the Manaslu granite and Tibetan Slab migmatites (Himalaya): insight in the origin and evolution of a crustal derived-granite magma. Chemical Geology 125, 1–17.

Barnicoat, A.C., Fry, N., 1986. High-pressure metamorphism of the Zermatt–Saas ophiolite zone, Switzerland. Journal of the Geological Society, London 143, 607–618.

Bearth, P., 1967. Die Ophiolithe der Zone von Zermatt–Saas-Fee. Stämpfli and Cie, Bern.

Belusova, E., Griffin, W.L., Pearson, N.J., 1998. Trace element composition and cathodoluminescence properties of southern African kimberlitic zircons. Mineralogical Magazine 62 (3), 355–366.

Buick, I.S., Cartwright, I., Harley, S.L., 1998. The retrograde $P-T-t$ path for the low-pressure granulites from the Reynolds Range, central Australia: petrological constraints and implications for low-P/high-T metamorphism. Journal of Metamorphic Geology 16, 511–530.

Buick, I., Frei, R., Cartwright, I., 1999. The timing of high-temperature retrogression in the Reynolds Range, central Australia: constraints from garnet and epidote Pb–Pb dating. Contributions to Mineralogy and Petrology 135, 244–254.

Cherniak, D.J., Watson, E.B., 2001. Pb diffusion in zircon. Chemical Geology 172, 5–24.

Clarke, G.L., Powell, R., 1991. Proterozoic granulite facies metamorphism in the southeastern Reynolds Range, central Australia: geological context, $P-T$ path and overprinting relationships. Journal of Metamorphic Geology 9, 267–281.

Compagnoni, R., 1977. The Sesia–Lanzo Zone: high pressure–low temperature metamorphism in the Austroalpine continental margin. Rendiconti della Societa Italiana di Mineralogia e Petrologia 33, 335–375.

Cornell, D.H., Scherstén, A., Hoskin, P., Lindsay, J., 1999. Application of charge-radius concepts to trace elements in igneous and metamorphic zircon. 9th Annual V.M. Goldschmidt Conference. Lunar and Planetary Institute, Cambridge, MA, pp. 61–62.

Dirks, P.H.G.M., Hand, M., Powell, R., 1991. The $P-T-$deformation path for a mid-Proterozoic, low pressure terrane: the Reynolds Range, central Australia. Journal of Metamorphic Geology 9, 641–661.

Dûchene, S., et al., 1997. The Lu–Hf dating of garnets the ages of the Alpine high-pressure metamorphism. Nature 387, 586–589.

Eggins, S.M., Rudnick, R.L., McDonough, W.F., 1998. The composition of peridotites and their minerals: a laser ablation ICP-MS study. Earth and Planetary Science Letters 154, 53–71.

Fraser, G., Ellis, D., Eggins, S., 1997. Zirconium abundance in granulite-facies minerals, with implications for zircon geochronology in high-grade rocks. Geology 25 (7), 607–610.

Fujimaki, H., 1986. Partition coefficients of Hf, Zr, REE between zircon, apatite and liquid. Contributions to Mineralogy and Petrology 94, 42–45.

Gebauer, D., Schertl, H.-P., Brix, M., Schreyer, W., 1997. 35 Ma old ultrahigh-pressure metamorphism and evidence for very rapid exhumation in the Dora Maira Massif, Western Alps. Lithos 41, 5–24.

Günther, D., Frischknecht, R., Heinrich, C.A., Kahlert, H.J., 1997. Capabilities of an argon fluoride 193nm Excimer Laser for laser ablation inductively coupled plasma mass spectrometry microanalysis of geological materials. Journal of Analytical Atomic Spectrometry 12, 939–944.

Heaman, L.M., Bowsin, R., Crocket, J., 1990. The chemical composition of igneous zircon suites: implications for geochemical tracer studies. Geochimica et Cosmochimica Acta 54, 1597–1607.

Hermann, J., Rubatto, D., Korsakov, A., Shatsky, V.S., 2001. Multiple zircon growth during fast exhumation of diamondiferous, deeply subducted continental crust (Kokchetav massif, Kazakhstan). Contributions to Mineralogy and Petrology 141, 66–82.

Hinton, R.W., Upton, B.G.J., 1991. The chemistry of zircon: variations within and between large crystals from syenite and alkali basalt xenoliths. Geochimica et Cosmochimica Acta 55, 3287–3302.

Hoskin, P.W.O., 1998. Minor and trace element analysis of natural zircon (ZrSiO4) by SIMS and laser ablation ICPMS: a consideration and comparison of two broadly competitive techniques. Journal of Trace and Microprobe Techniques 16 (3), 301–326.

Hoskin, P.W.O., Black, L.P., 2000. Metamorphic zircon formation by solid-state recrystallization of protolith igneous zircon. Journal of Metamorphic Geology 18, 423–439.

Hoskin, P.W.O., Ireland, T.R., 2000. Rare earth element chemistry of zircon and its use as a provenance indicator. Geology 28 (7), 627–630.

Inger, S., Ramsbotham, W., Cliff, R.A., Rex, D.C., 1996. Metamorphic evolution of the Sesia–Lanzo Zone, Western Alps: time constraints from multi-system geochronology. Contributions to Mineralogy and Petrology 126, 152–168.

Irvin, A.J., Frey, F.A., 1978. Distribution of trace elements between garnet megacrysts and host volcanic liquids of kimberlitic to rhyolitic composition. Geochimica et Cosmochimica Acta 42, 771–787.

Lee, J.K.W., Williams, I.S., Ellis, D.J., 1997. Pb, U and Th diffusion in natural zircon. Nature 390, 159–161.

Liati, A., Gebauer, D., 1999. Constraining the prograde and retrograde $P-T-$t path of Eocene HP rocks by SHRIMP dating different zircon domains: inferred rates of heating, burial, cooling and exhumation for central Rhodope, northern Greece. Contributions to Mineralogy and Petrology 135, 340–354.

Maas, R., Kinny, P.D., Williams, I.S., Froude, D.O., Compston, W., 1992. The Earth's oldest known crust: a geochronological and geochemical study of 3900–4200 Ma old detrital zircon from Mt. Narryer and Jack Hill, Western Australia. Geochimica et Cosmochimica Acta 56, 1281–1300.

Murali, A.V., Parthasarathy, R., Mahadevan, T.M., Sankar Das, M., 1983. Trace element characteristics, REE patterns and partition coefficients of zircons from different geological environments—A case study on Indian zircons. Geochimica et Cosmochimica Acta 47, 2047–2052.

Nagasawa, H., 1970. Rare earth concentrations in zircons and apatites and their host dacites and granites. Earth and Planetary Science Letters 9, 359–364.

Paterson, B.A., et al., 1992. The nature of zircon inheritance in two granitic plutons. Transactions of the Royal Society of Edinburgh Earth Sciences 83, 459–471.

Peucat, J.J., Hirata, T., Nesbitt, R.W., 1995. REE fractionation (ICPMS LASER) evidence in metamorphic zircons during granulite facies metamorphism and anatectic processes. Terra Abstracts 7 (Abstr. Suppl. 1), 346.

Pognante, U., 1989. Tectonic implications of lawsonite formation in the Sesia zone (western Alps). Tectonophysics 162, 219–227.

Ramsbotham, W., Inger, S., Cliff, B., Rex, D., Barnicoat, A., 1994. Time constraints on the metamorphic and structural evolution of the southern Sesia–Lanzo Zone, Western Italian Alps. Mineralogical Magazine 58A, 758–759.

Reinecke, T., 1991. Very high pressure metamorphism and uplift of coesite-bearing metasediments from the Zermatt–Saas zone Western Alps. European Journal of Mineralogy 3, 7–17.

Roberts, M.P., Finger, F., 1997. Do U–Pb zircon ages from granulites reflect peak metamorphic conditions? Geology 25 (4), 319–322.

Rubatto, D., Gebauer, D., 2000. Use of cathodoluminescence for U–Pb zircon dating by ion microprobe: some examples from the Western Alps. In: Pagel, M., Barbin, V., Blanc, P., Ohnenstetter, D. (Eds.), Cathodoluminescence in Geosciences. Springer, Berlin, pp. 373–400.

Rubatto, D., Gebauer, D., Fanning, M., 1998. Jurassic formation and Eocene subduction of the Zermatt–Saas-Fee ophiolites: implications for the geodynamic evolution of the Central and Western Alps. Contributions to Mineralogy and Petrology 132, 269–287.

Rubatto, D., Gebauer, D., Compagnoni, R., 1999. Dating of eclogite-facies zircons: the age of Alpine metamorphism in the Sesia–Lanzo Zone (Western Alps). Earth and Planetary Science Letters 167, 141–158.

Rubatto, D., Williams, I.S., Buick, I.S., 2001. Zircon and monazite response to prograde metamorphism in the Reynolds Range, central Australia. Contributions to Mineralogy and Petrology 140, 458–468.

Schaltegger, U., Fanning, M., Günther, D., Maurin, J.C., Schulmann, K., Gebauer, D., 1999. Growth, annealing and recrystallization of zircon and preservation of monazite in high-grade metamorphism: conventional and in-situ U–Pb isotope, cathodoluminescence and microchemical evidence. Contributions to Mineralogy and Petrology 134, 186–201.

Schnetzler, C.C., Philpotts, J.P., 1970. Partition coefficients of rare-earth elements between igneous matrix material and rock forming mineral phenocrysts—II. Geochimica et Cosmochimica Acta 34, 331–340.

Scoates, J.S., Chamberlain, K.R., 1997. Orogenic to post-orogenic origin for the 1.76 Ga Horse Creek anorthosite complex, Wyoming, USA. The Journal of Geology 105, 243–331.

Sisson, T.W., Bacon, R., 1992. Garnet/high-silica rhyolite trace element partition coefficients measured by ion microprobe. Geochimica et Cosmochimica Acta 56, 2133–2136.

Sun, S.S., McDonough, W.F., 1989. Chemical and isotopic systematics of oceanic basalts: implications for mantle composition and processes. In: Sanders, A.D., Norry, M.J. (Eds.), Magmatism in the Ocean Basins. Geological Society of London Special Publication, vol. 42, 313–345.

Vry, J., Compston, W., Cartwright, I., 1996. SHRIMP II dating of zircons and monazites: reassessing the timing of high-grade metamorphism and fluid flow in the Reynolds Range, northern Arunta Block Australia. Journal of Metamorphic Geology 14, 335–350.

Watson, B.E., 1980. Some experimentally determined zircon/liquid partition coefficients for the rare earth elements. Geochimica et Cosmochimica Acta 44, 895–897.

Williams, I.S., Buick, I.S., Cartwright, I., 1996. An extended episode of early Mesoproterozoic metamorphic fluid flow in the Reynolds Range, central Australia. Journal of Metamorphic Geology 14, 29–47.